Optical tweezers computational toolbox

7 AUTHORS, INCLUDING:

Vincent Loke
University of Queensland

48 PUBLICATIONS **386** CITATIONS

SEE PROFILE

Alexander B. Stilgoe
University of Queensland

29 PUBLICATIONS **316** CITATIONS

SEE PROFILE

Halina Rubinsztein-Dunlop
University of Queensland

341 PUBLICATIONS **5,763** CITATIONS

SEE PROFILE

Optical tweezers computational toolbox

**Timo A Nieminen, Vincent L Y Loke, Alexander B Stilgoe,
Gregor Knöner, Agata M Brańczyk, Norman R Heckenberg
and Halina Rubinsztein-Dunlop**

Centre for Biophotonics and Laser Science, School of Physical Sciences, The
University of Queensland, Brisbane QLD 4072, Australia

Abstract. We describe a toolbox, implemented in Matlab, for the computational
modelling of optical tweezers. The toolbox is designed for the calculation of optical
forces and torques, and can be used for both spherical and nonspherical particles, in
both Gaussian and other beams. The toolbox might also be useful for light scattering
using either Lorenz–Mie theory or the T-matrix method.

1. Introduction

Computational modelling provides an important bridge between theory and
experiment—apart from the simplest cases, computational methods must be used
to obtain quantitative results from theory for comparison with experimental results.
This is very much the case for optical trapping, where the size range of typical
particles trapped and manipulated in optical tweezers occupies the gap between the
geometric optics and Rayleigh scattering regimes, necessitating the application of
electromagnetic theory. Although, in principle, the simplest cases—the trapping and
manipulation of homogeneous and isotropic microspheres—has an analytical solution—
generalised Lorenz–Mie theory—significant computational effort is still required to
obtain quantitative results. Unfortunately, the mathematical complexity of Lorenz–
Mie theory presents a significant barrier to entry for the novice, and is likely to be a
major contributor to the lagging of rigorous computational modelling of optical tweezers
compared to experiment.

If we further consider the calculation of optical forces and torques on non-
spherical particles—for example, if we wish to consider optical torques on and rotational
alignment of non-spherical microparticles, the mathematical difficulty is considerably
greater. Interestingly, one of the most efficient methods for calculating optical forces

and torques on non-spherical particles in optical traps is closly allied to Lorenz–Mie theory—the T-matrix method (Waterman 1971, Mishchenko 1991, Nieminen et al. 2003a). However, while the Mie scattering coefficients have a relatively simple analytical form, albeit involving special functions, the T-matrix requires considerable numerical effort for its calculation. It is not surprising that the comprehensive bibliographic database on computational light scattering using the T-matrix method by Mishchenko et al. (2004) lists only four papers applying the method to optical tweezers (Bayoudh et al. 2003, Bishop et al. 2003, Nieminen, Rubinsztein-Dunlop, Heckenberg & Bishop 2001, Nieminen, Rubinsztein-Dunlop & Heckenberg 2001). Since the compilation of this bibliography, other papers have appeared in which this is done (Nieminen et al. 2004, Simpson & Hanna 2007, Singer et al. 2006), but they are few in number.

Since the potential benefits of precise and accurate computational modelling of optical trapping is clear, both for spherical and non-spherical particles, we believe that the release of a freely-available computational toolbox will be valuable to the optical trapping community.

We describe such a toolbox, implemented in Matlab. We outline the theory underlying the computational methods, the mathematics and the algorithms, the toolbox itself, typical usage, and present some example results. The toolbox can be obtained at http://www.physics.uq.edu.au/people/nieminen/software.html at the time of publication. Since such software projects tend to evolve over time, and we certainly intend that this one will do so, potential users are advised to check the accompanying documentation. Along these lines, we describe our plans for future development. Of course, we welcome input, feedback, and contributions from the optical trapping community.

2. Fundamentals

The optical forces and torques that allow trapping and manipulation of microparticles in beams of light result from the transfer of momentum and angular momentum from the electromagnetic field to the particle—the particle alters the momentum or angular momentum flux of the beam through scattering. Thus, the problem of calculating optical forces and torques is essentially a problem of computational light scattering. In some ways, it is a simple problem: the incident field is monochromatic, there is usually only a single trapped particle, which is finite in extent, and speeds are so much smaller than the speed of light that we can for most purposes neglect Doppler shifts and assume we have a steady-state monochromatic single-scattering problem.

Although typical particles inconveniently are of sizes lying within the gap between the regimes of applicability of small-particle approximations (Rayleigh scattering) and large-particle approximations (geometric optics), the particles of choice are often homogeneous isotropic spheres, for which an analytical solution to the scattering problem is available—the Lorenz–Mie solution (Lorenz 1890, Mie 1908). While the

application of Lorenz–Mie theory requires significant computational effort, the methods are well-known.

The greatest difficulty encountered results from the incident beam being a tightly focussed beam. The original Lorenz–Mie theory was developed for scattering of plane waves, and its extension to non-plane illumination is usually called generalised Lorenz–Mie theory (GLMT) (Gouesbet & Grehan 1982) which has seen significant use for modelling the optical trapping of homogeneous isotropic spheres (Ren et al. 1996, Wohland et al. 1996, Maia Neto & Nussenzweig 2000, Mazolli et al. 2003, Lock 2004*a*, Lock 2004*b*, Knöner et al. 2006, Neves et al. 2006). The same name is sometimes used for the extension of Lorenz–Mie theory to non-spherical, but still separable geometries such as spheroids (Han & Wu 2001, Han et al. 2003).

The source of the difficulty lies in the usual paraxial representations of laser beams being solutions of the scalar paraxial wave equation rather than solutions of the vector Helmholtz equation. Our method of choice is to use a least-squares fit to produce a Helmholtz beam with a far-field matching that expected from the incident beam being focussed by the objective (Nieminen et al. 2003*b*).

At this point, we can write the incident field in terms of a discrete basis set of functions $\psi_n^{(\mathrm{inc})}$, where n is mode index labelling the functions, each of which is a solution of the Helmholtz equation,

$$U_{\mathrm{inc}} = \sum_n^\infty a_n \psi_n^{(\mathrm{inc})}, \tag{1}$$

where a_n are the expansion coefficients for the incident wave. In practice, the sum must be truncated at some finite $n_{\max}$, which places restrictions on the convergence behaviour of useful basis sets. A similar expansion is possible for the scattered wave, and we can write

$$U_{\mathrm{scat}} = \sum_k^\infty p_k \psi_k^{(\mathrm{scat})}, \tag{2}$$

where p_k are the expansion coefficients for the scattered wave.

As long as the response of the scatterer—the trapped particle in this case—is linear, the relation between the incident and scattered fields must be linear, and can be written as a simple matrix equation

$$p_k = \sum_n^\infty T_{kn} a_n \tag{3}$$

or, in more concise notation,

$$\mathbf{P} = \mathbf{TA} \tag{4}$$

where T_{kn} are the elements of the T-matrix. This is the foundation of both GLMT and the T-matrix method. In GLMT, the T-matrix $\mathbf{T}$ is diagonal, whereas for non-spherical particles, it is not.

When the scatterer is finite and compact, the most useful set of basis functions is vector spherical wavefunctions (VSWFs) (Waterman 1971, Mishchenko 1991, Nieminen

et al. 2003a, Nieminen et al. 2003b). Since the VSWFs are a discrete basis, this method lends itself well to representation of the fields on a digital computer, especially since their convergence is well-behaved and known (Brock 2001).

The T-matrix depends only on the properties of the particle—its composition, size, shape, and orientation—and the wavelength, and is otherwise independent of the incident field. This means that for any particular particle, the T-matrix only needs to be calculated once, and can then be used for repeated calculations of optical force and torque. This is the key point that makes this a highly attractive method for modelling optical trapping and micromanipulation, since we are typically interested in the optical force and torque as a function of position within the trap, even if we are merely trying to find the equilibrium position and orientation within the trap. Thus, calculations must be performed for varying incident illumination, which can be done very easily with the T-matrix method. This provides a significant advantage over many other methods of calculating scattering where the entire calculation needs to be repeated. This is perhaps the the reason that while optical forces and torques have been successfully modelled using methods such as the finite-difference time-domain method (FDTD), the finite element method (FEM), or other methods (White 2000b, White 2000a, Hoekstra et al. 2001, Collett et al. 2003, Gauthier 2005, Chaumet et al. 2005, Sun et al. 2006, Wong & Ratner 2006), the practical application of such work has been limited.

Since, as noted above, the optical forces and torques result from differences between the incoming and outgoing fluxes of electromagnetic momentum and angular momentum, calculation of these fluxes is required. This can be done by integration of the Maxwell stress tensor, and its moment for the torque, over a surface surrounding the particle. Fortunately, in the T-matrix method, the bulk of this integral can be performed analytically, exploiting the orthogonality properties of the VSWFs. In this way, the calculation can be reduced to sums of products of the expansion coefficients of the fields.

At this point, two controversies in macroscopic classical electromagnetic theory intrude. The first of these is the Abraham–Minkowski controversy, concerning the momentum of an electromagnetic wave in a material medium (Minkowski 1908, Abraham 1909, Abraham 1910, Jackson 1999, Pfeifer et al. 2006). This controversy is resolved for practical purposes by the realisation that what is physically observable is not the force due to change in the *electromagnetic* momentum, but the force due to the *total* momentum. The controversy is essentially one of semantics—what portion of the total momentum is to be labelled "electromagnetic", and what portion is to be labelled "material" (Pfeifer et al. 2006). Abraham's approach can be summarised as calling P/nc the electromagnetic momentum flux, where P is the power, n the refractive index, and c the speed of light in free space. The quantum equivalent is the momentum of a photon in a material medium being $\hbar k/n^2 = \hbar k_0/n$. Minkowski, on the other hand, gives nP/c as the electromagnetic momentum flux, or $\hbar k = n\hbar k_0$ per photon. The discrepancy is resolved by realising that the wave of induced polarisation in the dielectric carries energy and momentum, equal to the difference between the Abraham and Minkowski

pictures. It is simplest to use the Minkowski momentum flux nP/c, since this is equal to the total momentum flux.

The second controversy is the angular momentum density of circularly polarised electromagnetic waves (Humblet 1943, Khrapko 2001, Zambrini & Barnett 2005, Stewart 2005, Pfeifer et al. 2006). On the one hand, we can begin with the assumption that the angular momentum density is the moment of the momentum density, $r \times (\mathbf{E} \times \mathbf{H})/c$, which results in a circularly polarised plane wave carrying zero angular momentum in the direction of propagation. On the other hand, we can begin with the Lagrangian for an electromagnetic radiation field, and obtain the canonical stress tensor and an angular momentum tensor that can be divided into spin and orbital components (Jauch & Rohrlich 1976). For a circularly polarised plane wave, the component of the angular momentum flux in the direction of propagation would be I/ω, where I is the irradiance and ω the angular frequency, in disagreement with the first result. The division of the angular momentum density resulting from this procedure is not gauge-invariant, and it is common to transform the integral of the angular momentum density into a gauge-invariant form, yielding the integral of $r \times (\mathbf{E} \times \mathbf{H})/c$. Jauch & Rohrlich (1976) carefully point out that this transformation requires the dropping of surface terms at infinity. The reverse of this procedure, obtaining the spin and orbital term starting from $r \times (\mathbf{E} \times \mathbf{H})/c$, involving the same surface terms, had already been shown by Humblet (1943). The controversy thus consists of which of the two possible integrands to call the angular momentum density.

However, it is not the angular momentum density as such that we are interested in, but the total angular momentum flux through a spherical surface surrounding the particle. For the electromagnetic fields used in optical tweezers, this integrated flux is the same for both choices of angular momentum density. Crichton & Marston (2000) also show that for monochromatic radiation, the division into spin and orbital angular momenta is gauge-invariant, and observable, with it being possible to obtain the spin from measurement of the Stokes parameters. The total angular momentum flux is the same as that resulting from assuming a density of $r \times (\mathbf{E} \times \mathbf{H})/c$. Since the torque due to spin is of practical interest (Nieminen, Heckenberg & Rubinsztein-Dunlop 2001, Bishop et al. 2003, Bishop et al. 2004), it is worthwhile to calculate this separately from the total torque.

3. Incident field

The natural choice of coordinate system for optical tweezers is spherical coordinates centered on the trapped particle. Thus, the incoming and outgoing fields can be expanded in terms of incoming and outgoing vector spherical wavefunctions (VSWFs):

$$\mathbf{E}_{\text{in}} = \sum_{n=1}^{\infty} \sum_{m=-n}^{n} a_{nm}\mathbf{M}_{nm}^{(2)}(k\mathbf{r}) + b_{nm}\mathbf{N}_{nm}^{(2)}(k\mathbf{r}), \tag{5}$$

$$\mathbf{E}_{\text{out}} = \sum_{n=1}^{\infty} \sum_{m=-n}^{n} p_{nm}\mathbf{M}_{nm}^{(1)}(k\mathbf{r}) + q_{nm}\mathbf{N}_{nm}^{(1)}(k\mathbf{r}). \tag{6}$$

where the VSWFs are

$$\mathbf{M}_{nm}^{(1,2)}(k\mathbf{r}) = N_n h_n^{(1,2)}(kr)\mathbf{C}_{nm}(\theta,\phi) \tag{7}$$

$$\mathbf{N}_{nm}^{(1,2)}(k\mathbf{r}) = \frac{h_n^{(1,2)}(kr)}{krN_n}\mathbf{P}_{nm}(\theta,\phi) + N_n\left(h_{n-1}^{(1,2)}(kr) - \frac{nh_n^{(1,2)}(kr)}{kr}\right)\mathbf{B}_{nm}(\theta,\phi)$$

where $h_n^{(1,2)}(kr)$ are spherical Hankel functions of the first and second kind, $N_n = [n(n+1)]^{-1/2}$ are normalization constants, and $\mathbf{B}_{nm}(\theta,\phi) = \mathbf{r}\nabla Y_n^m(\theta,\phi)$, $\mathbf{C}_{nm}(\theta,\phi) = \nabla \times (\mathbf{r}Y_n^m(\theta,\phi))$, and $\mathbf{P}_{nm}(\theta,\phi) = \hat{\mathbf{r}}Y_n^m(\theta,\phi)$ are the vector spherical harmonics (Waterman 1971, Mishchenko 1991, Nieminen et al. 2003a, Nieminen et al. 2003b), and $Y_n^m(\theta,\phi)$ are normalized scalar spherical harmonics. The usual polar spherical coordinates are used, where θ is the co-latitude measured from the $+z$ axis, and ϕ is the azimuth, measured from the $+x$ axis towards the $+y$ axis.

$\mathbf{M}_{nm}^{(1)}$ and $\mathbf{N}_{nm}^{(1)}$ are outward-propagating TE and TM multipole fields, while $\mathbf{M}_{nm}^{(2)}$ and $\mathbf{N}_{nm}^{(2)}$ are the corresponding inward-propagating multipole fields. Since these wavefunctions are purely incoming and purely outgoing, each has a singularity at the origin. Since fields that are free of singularities are of interest, it is useful to define the singularity-free regular vector spherical wavefunctions:

$$\mathbf{RgM}_{nm}(k\mathbf{r}) = \tfrac{1}{2}[\mathbf{M}_{nm}^{(1)}(k\mathbf{r}) + \mathbf{M}_{nm}^{(2)}(k\mathbf{r})], \tag{8}$$

$$\mathbf{RgN}_{nm}(k\mathbf{r}) = \tfrac{1}{2}[\mathbf{N}_{nm}^{(1)}(k\mathbf{r}) + \mathbf{N}_{nm}^{(2)}(k\mathbf{r})]. \tag{9}$$

Although it is usual to expand the incident field in terms of the regular VSWFs, and the scattered field in terms of outgoing VSWFs, this results in both the incident and scattered waves carrying momentum and angular momentum away from the system. Since we are primarily interested in the transport of momentum and angular momentum by the fields (and energy, too, if the particle is absorbing), we separate the total field into purely incoming and outgoing portions in order to calculate these. The user of the code can choose whether the incident–scattered or incoming–outgoing representation is used otherwise.

We use an over-determined point-matching scheme to find the expansion coefficients a_{nm} and b_{nm} describing the incident beam (Nieminen et al. 2003b), providing stable and robust numerical performance and convergence.

Finally, one needs to be able to calculate the force and torque for the same particle in the same trapping beam, but at different positions or orientations. The transformations of the VSWFs under rotation of the coordinate system or translation of the origin of the coordinate system are known (Brock 2001, Videen 2000, Gumerov & Duraiswami 2003, Choi et al. 1999). It is sufficient to find the VSWF expansion of the incident beam for a single origin and orientation, and then use translations and rotations to find the new VSWF expansions about other points (Nieminen et al. 2003b, Doicu & Wriedt 1997). Since the transformation matrices for rotation and translations along the z-axis are sparse, while the transformation matrices for arbitrary translations are full, the most efficient way to carry out an arbitrary translation is by a combination of rotation and axial translation. The transformation matrices for both rotations and axial

translations can be efficiently computed using recursive methods (Videen 2000, Gumerov & Duraiswami 2003, Choi et al. 1999).

3.1. Implementation

Firstly, it is necessary to provide routines to calculate the special functions involved. These include:

(i) `sbesselj.m`, `sbesselh.m`, `sbesselh1.m`, and `sbesselh2.m` for the calculation of spherical Bessel and Hankel functions. These make use of the Matlab functions for cylindrical Bessel functions.

(ii) `spharm.m` for scalar spherical harmonics and their angular partial derivatives.

(iii) `vsh.m` for vector spherical harmonics.

(iv) `vswf.m` for vector spherical wavefunctions.

Secondly, routines must be provided to find the expansion coefficients, or beam shape coefficients, a_{nm} and b_{nm} for the trapping beam. These are:

(i) `bsc_pointmatch_farfield.m` and `bsc_pointmatch_focalplane.m`, described in (Nieminen et al. 2003*b*), which can calculate the expansion coefficients for Gaussian beams, Laguerre–Gauss modes, and bi-Gaussian beams. Since these routines are much faster for rotationally symmetric beams, such as Laguerre–Gauss beams, a routine, `lgmodes.m`, that can provide the Laguerre–Gauss decomposition of an arbitrary paraxial beam is also provided.

(ii) `bsc_plane.m`, for the expansion coefficients of a plane wave. This is not especially useful for optical trapping, but makes the toolbox more versatile, improving its usability for more general light scattering calculations.

Thirdly, the transformation matrices for the expansion coefficients under rotations and translations must be calculated. Routines include:

(i) `wigner_rotation_matrix.m`, implementing the algorithm given by Choi et al. (1999).

(ii) `translate_z.m`, implementing the algorithm given by Videen (2000).

4. *T*-matrix

For spherical particles, the usual Mie coefficients can be rapidly calculated. For non-spherical particles, a more intensive numerical effort is required. We use a least-squares overdetermined point-matching method (Nieminen et al. 2003*a*). For axisymmetric particles, the method is relatively fast. However, as is common for many methods of calculating the *T*-matrix, particles cannot have extreme aspect ratios, and must be simple in shape. Typical particle shapes that we have used are spheroids and cylinders, and aspect ratios of up to 4 give good results. Although general non-axisymmetric particles can take a long time to calculate the *T*-matrix for, it is possible to make

use of symmetries such as mirror symmetry and discrete rotational symmetry to greatly speed up the calculation (Kahnert 2005, Nieminen et al. 2006). We include a symmetry-optimised T-matrix routine for cubes.

Expanding the range of particles for which we can calculate the T-matrix is one of our current active research efforts, and we plan to include routines for anistropic and inhomogeneous particles, and particles with highly complex geometries.

Once the T-matrix is calculated, the scattered field coefficients are simply found by a matrix–vector multiplication of the T-matrix and a vector of the incident field coefficients.

4.1. Implementation

Our T-matrix routines include:

 (i) `tmatrix_mie.m`, calculating the Mie coefficients for homogeneous isotropic spheres.
 (ii) `tmatrix_pm.m`, our general point-matching T-matrix routine.
(iii) `tmatrix_pm_cube.m`, the symmetry-optimised cube code.

5. Optical force and torque

As noted earlier, the integrals of the momentum and angular momentum fluxes reduce to sums of products of the expansion coefficients. It is sufficient to give the formulae for the z-components of the fields, as given, for example, by Crichton & Marston (2000). We use the same formulae to calculate the x and y components of the optical force and torque, using $90°$ rotations of the coordinate system (Choi et al. 1999). It is also possible to directly calculate the x and y components using similar, but more complicated, formulae (Farsund & Felderhof 1996).

The axial trapping efficiency Q is

$$
\begin{aligned}
Q = \frac{2}{P} \sum_{n=1}^{\infty} \sum_{m=-n}^{n} & \frac{m}{n(n+1)} \mathrm{Re}(a_{nm}^{\star} b_{nm} - p_{nm}^{\star} q_{nm}) \\
& - \frac{1}{n+1} \left[\frac{n(n+2)(n-m+1)(n+m+1)}{(2n+1)(2n+3)} \right]^{\frac{1}{2}} \\
& \times \mathrm{Re}(a_{nm} a_{n+1,m}^{\star} + b_{nm} b_{n+1,m}^{\star} \\
& \quad - p_{nm} p_{n+1,m}^{\star} - q_{nm} q_{n+1,m}^{\star})
\end{aligned}
\tag{10}
$$

in units of $n\hbar k$ per photon, where n is the refractive index of the medium in which the trapped particles are suspended. This can be converted to SI units by multiplying by nP/c, where P is the beam power and c is the speed of light in free space.

The *torque efficiency*, or normalized torque, about the z-axis acting on a scatterer is

$$
\tau_z = \sum_{n=1}^{\infty} \sum_{m=-n}^{n} m(|a_{nm}|^2 + |b_{nm}|^2 - |p_{nm}|^2 - |q_{nm}|^2)/P
\tag{11}
$$

in units of $\hbar$ per photon, where

$$P = \sum_{n=1}^{\infty} \sum_{m=-n}^{n} |a_{nm}|^2 + |b_{nm}|^2 \tag{12}$$

is proportional to the incident power (omitting a unit conversion factor which will depend on whether SI, Gaussian, or other units are used). This torque includes contributions from both spin and orbital components, which can both be calculated by similar formulae (Crichton & Marston 2000). Again, one can convert these values to SI units by multiplying by P/ω, where ω is the optical frequency.

5.1. Implementation

One routine, `forcetorque.m`, is provided for the calculation of the force, torque and spin transfer. The orbital angular momentum transfer is the difference between the torque and the spin transfer. The incoming and outgoing power (the difference being the absorbed power) can be readily calculated directly from the expansion coefficients, as can be seen from (12).

6. Miscellaneous routines

A number of other routines that do not fall into the above categories are included. These include:

 (i) Examples of use.
(ii) Routines for conversion of coordinates and vectors from Cartesian to spherical and spherical to Cartesian.
(iii) Routines to automate common tasks, such as finding the equilibrium position of a trapped particle, spring constants, and force maps.
(iv) Functions required by other routines.

7. Typical use of the toolbox

Typically, for a given trap and particle, a T-matrix routine (usually `tmatrix_mie.m`) will be run once. Next, the expansion coefficients for the beam are found. Depending on the interests of the user, a function automating some common task, such as finding the equilibrium position within the trap, might be used, or the user might directly use the rotation and translation routines to enable calculation of the force or torque at desired positions within the trap.

The speed of calculation depends on the size of the beam, the size of the particle, and the distance of the particle from the focal point of the beam. Even for a wide beam and a large distance, the force and torque at a particular position can typically be calculated in much less than one second.

(a)

(b)
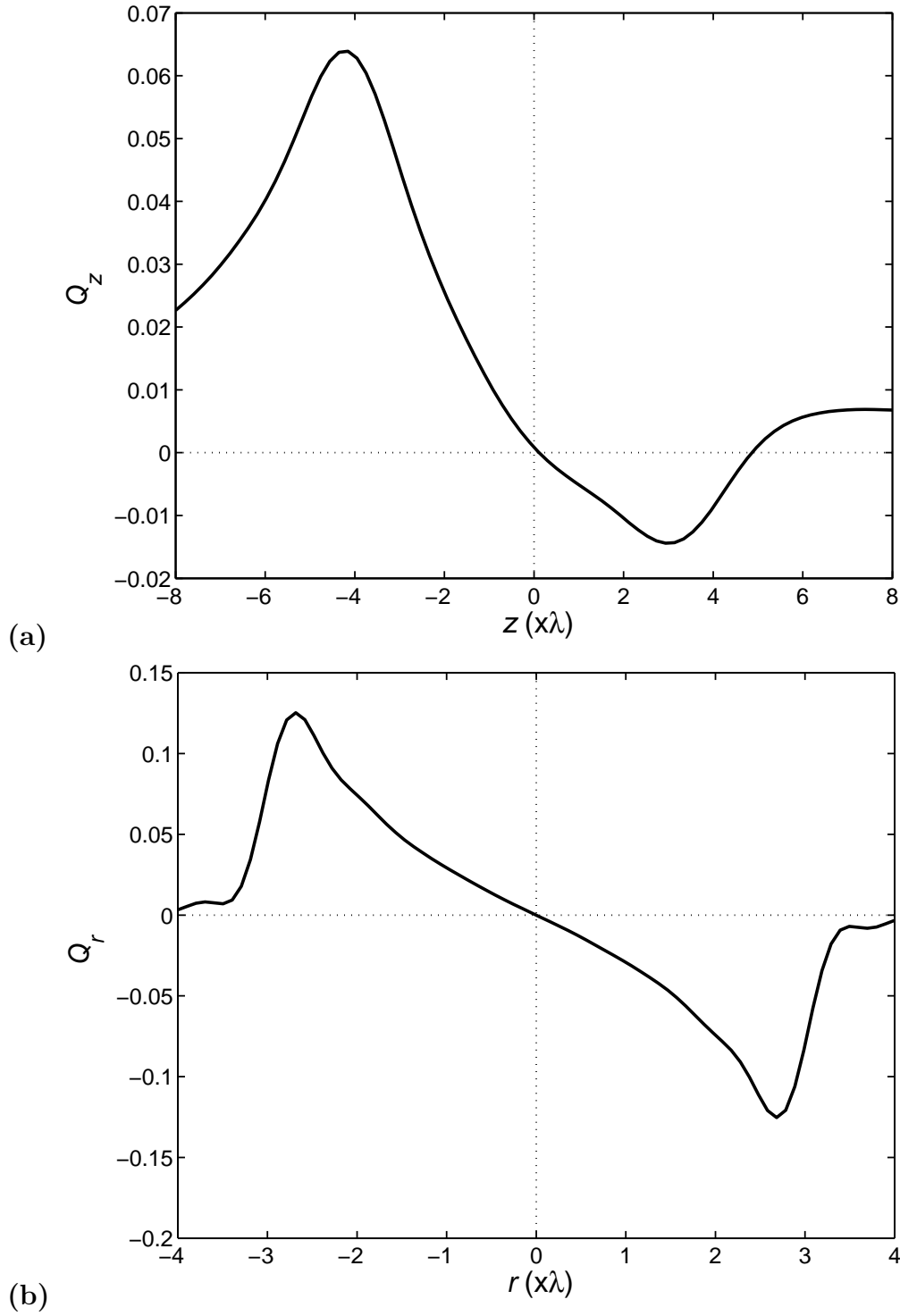
Figure 1. Gaussian trap (`example_gaussian.m`). Force on a sphere in a Gaussian beam trap. The half-angle of convergence of the $1/e^2$ edge of the beam is $50°$, corresponding to a numerical aperture of 1.02. The particle has a relative refractive index equal to $n = 1.59$ in water, and has a radius of 2.5λ, corresponding to a diameter of 4.0μm if trapped at $1064\,$nm in water. (a) shows the axial trapping efficiency as a function of axial displacement and (b) shows the transverse trapping efficiency as a function of transverse displacement from the equilibrium point.

(a)

(b)
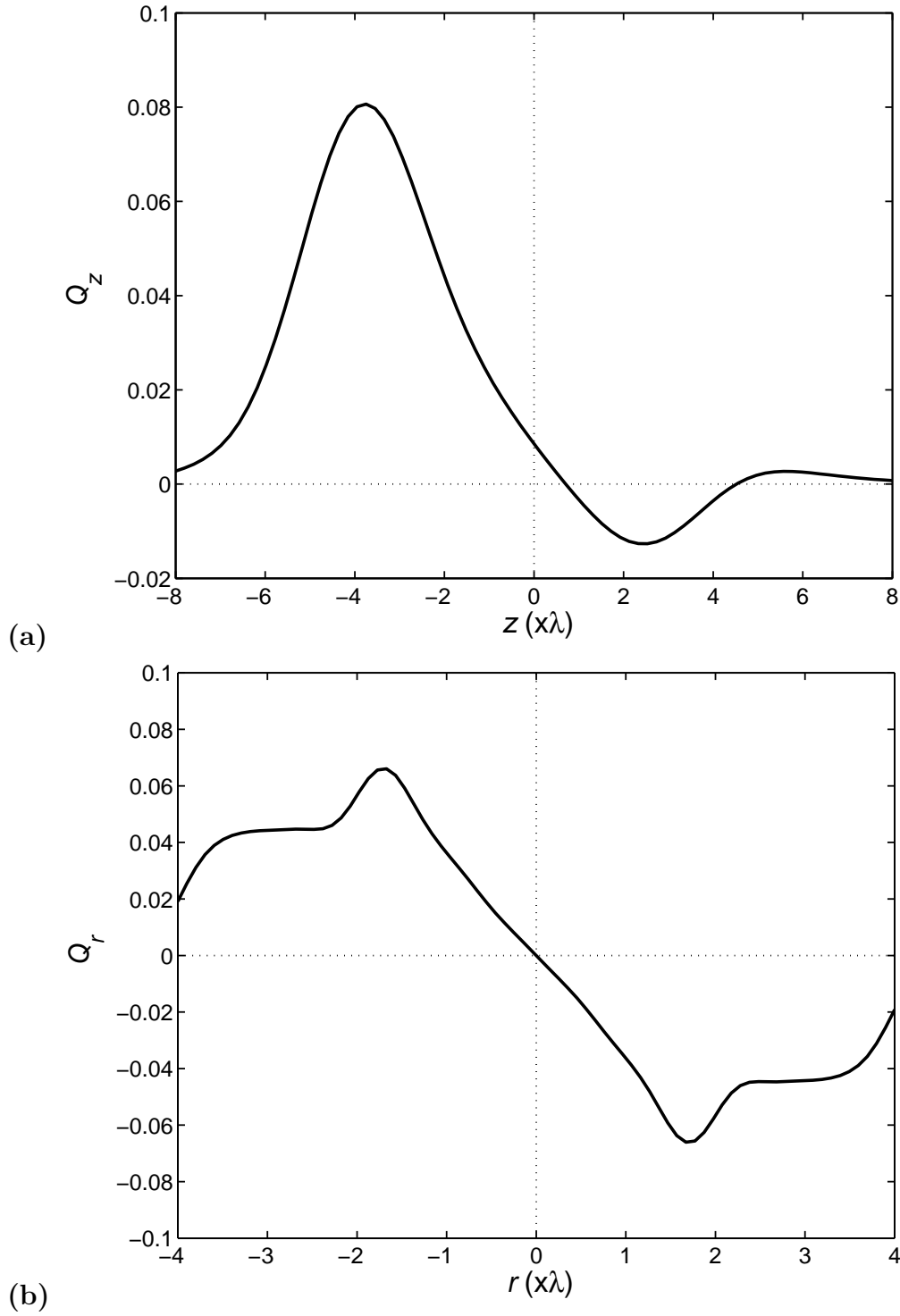
Figure 2. Laguerre–Gauss trap (`example_lg.m`). Force on a sphere in a Laguerre–Gauss beam trap. The half-angle of convergence of the $1/e^2$ outer edge of the beam is 50°, as in figure 1. The sphere is identical to that in figure 1. (a) shows the axial trapping efficiency as a function of axial displacement and (b) shows the transverse trapping efficiency as a function of transverse displacement from the equilibrium point. Compared with the Gaussian beam trap, the radial force begins to drop off at smaller radial displacements, due the far side of the ring-shaped beam no longer interacting with the particle.
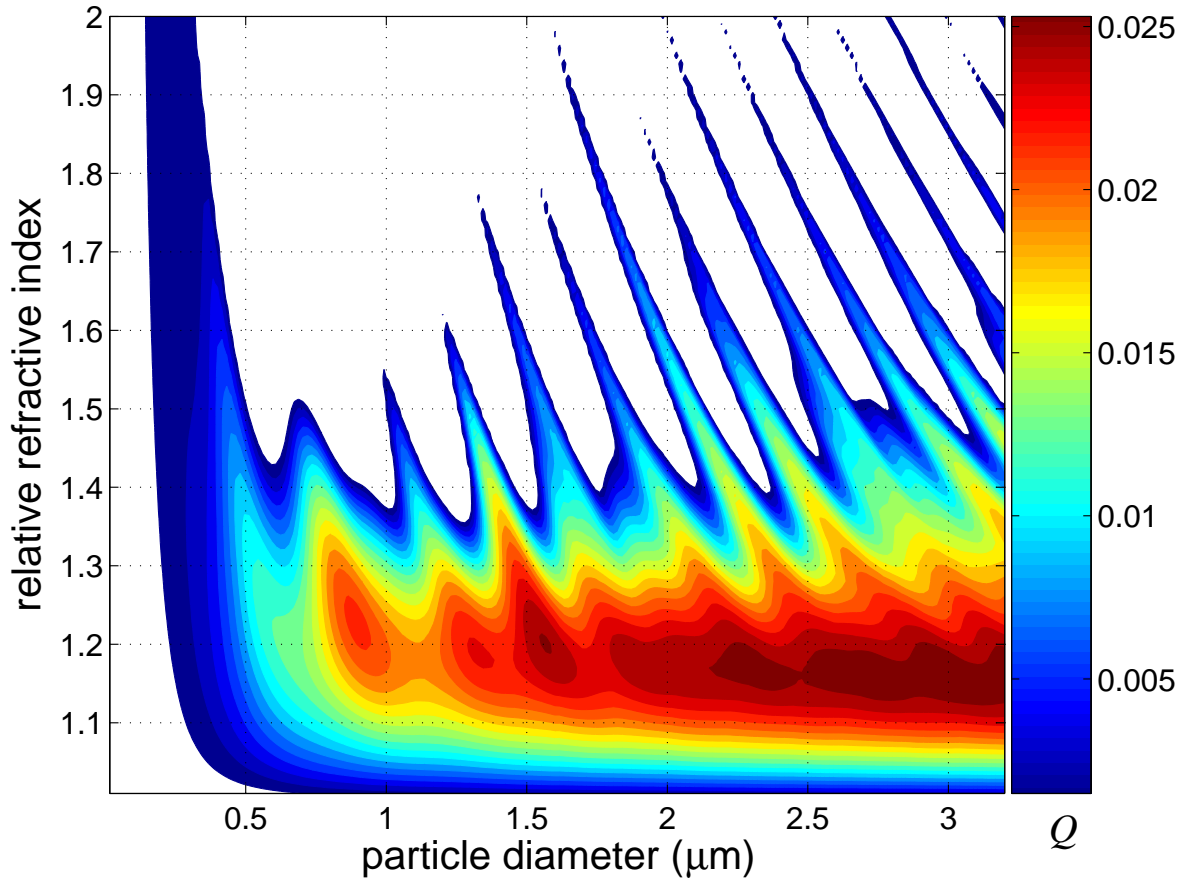
Figure 3. Trapping landscape (`example_landscape.m`). The maximum axial restoring force for displacement in the direction of beam propagation is shown, in terms of the trapping efficiency as a function of relative refractive index and microsphere diameter. The trapping beam is at 1064 nm and is focussed by an NA = 1.2 objective. This type of calculation is quite slow, as the trapping force as a function of axial displacement must be found for a grid of combinations of relative refractive index and sphere diameter. At the left-hand side, we can see that the trapping force rapidly becomes very small as the particle size becomes small—the gradient force is proportional to the volume of the particle for small particles. In the upper portion, we can see that whether or not the particle can be trapped strongly depends on the size—for particular sizes, reflection is minimised, and even high index particles can be trapped.

More complex tasks are possible, such as finding the optical force as a function of some property of the particle, which can, for example, be used to determine the refractive index of a microsphere (Knöner et al. 2006).

Figures 1 to 4 demonstrate some of the capabilities of the toolbox. Figure 1 shows a simple application—the determination of the force as a function of axial displacement from the equilibrium position in a Gaussian beam trap. Figure 2 shows a similar result, but for a particle trapped in a Laguerre–Gauss LG_{03} beam. Figure 3 shows a more complex application, with repeated calculations (each similar to the one shown in figure 1(a)) being used to determine the effect of the combination of relative refractive index and particle size on trapping. Finally, figure 4 shows the trapping of a non-spherical
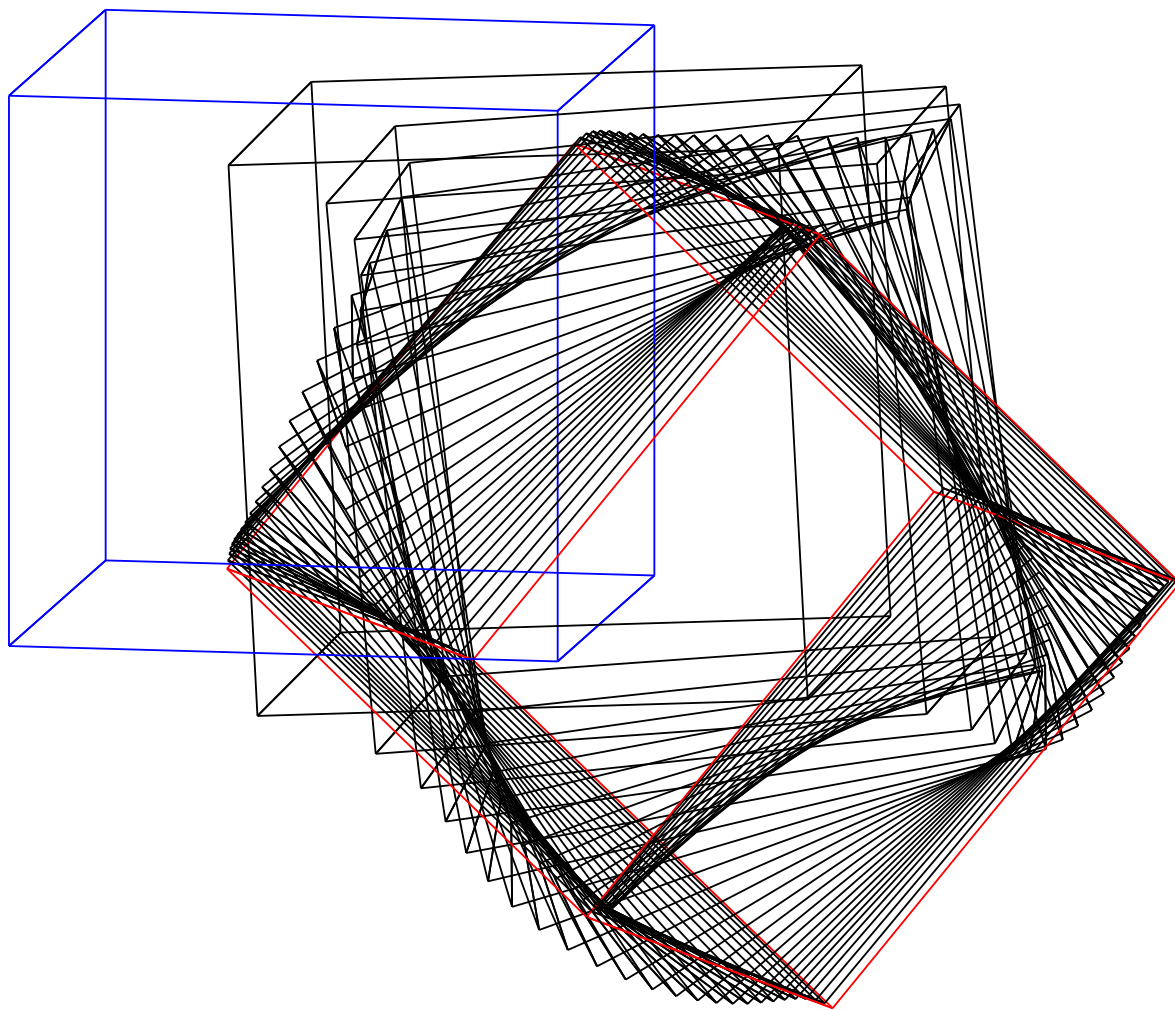
Figure 4. Optical trapping of a cube (`example_cube.m`). A sequence showing the optical trapping of a cube. The cube has faces of $2\lambda/n_{\mathrm{medium}}$ across, and has a refractive index of $n = 1.59$, and is trapped in water. Since the force and torque depend on the orientation as well as position, a simple way to find the equilibrium position and orientation is to "release" the cube and calculate the change in position and orientation for appropriate time steps. The cube can be assumed to always be moving at terminal velocity and terminal angular velocity (Nieminen, Rubinsztein-Dunlop, Heckenberg & Bishop 2001). The cube begins face-up, centred on the focal plane of the beam, and to one side. The cube is pulled into the trap and assumes a corner-up orientation. The symmetry optimisations allow the calculation of the T-matrix in 20 minutes; otherwise, 30 hours would be required. Once the T-matrix is found, successive calculations of the force and torque require far less time, on the order of a second or so.

particle, a cube.

Agreement with precision experimental measurements suggests that errors of less than 1% are expected.

8. Future development

We are actively engaged in work to extend the range of particles for which we can model trapping. This currently included birefringent particles and particles of arbitrary geometry. Routines to calculate the T-matrices for such particles will be included in the main code when available.

Other areas in which we aim to further improve the toolbox are robust handling of incorrect or suspect input, more automation of tasks, and GUI tools.

We also expect feedback from the optical trapping and micromanipulation community to help us add useful routines and features.

References

Abraham M 1909 *Rendiconti Circolo Matematico di Palermo* **28**, 1–28.

Abraham M 1910 *Rendiconti Circolo Matematico di Palermo* **30**, 33–46.

Bayoudh S, Nieminen T A, Heckenberg N R & Rubinsztein-Dunlop H 2003 *Journal of Modern Optics* **50**(10), 1581–1590.

Bishop A I, Nieminen T A, Heckenberg N R & Rubinsztein-Dunlop H 2003 *Physical Review A* **68**, 033802.

Bishop A I, Nieminen T A, Heckenberg N R & Rubinsztein-Dunlop H 2004 *Physical Review Letters* **92**(19), 198104.

Brock B C 2001 Using vector spherical harmonics to compute antenna mutual impedance from measured or computed fields Sandia report SAND2000-2217-Revised Sandia National Laboratories Albuquerque, New Mexico, USA.

Chaumet P C, Rahmani A, Sentenac A & Bryant G W 2005 *Physical Review E* **72**, 046708.

Choi C H, Ivanic J, Gordon M S & Ruedenberg K 1999 *Journal of Chemical Physics* **111**, 8825–8831.

Collett W L, Ventrice C A & Mahajan S M 2003 *Applied Physics Letters* **82**(16), 2730–2732.

Crichton J H & Marston P L 2000 *Electronic Journal of Differential Equations* **Conf. 04**, 37–50.

Doicu A & Wriedt T 1997 *Applied Optics* **36**, 2971–2978.

Farsund Ø & Felderhof B U 1996 *Physica A* **227**, 108–130.

Gauthier R C 2005 *Optics Express* **13**(10), 3707–3718.

Gouesbet G & Grehan G 1982 *Journal of Optics (Paris)* **13**(2), 97–103.

Gumerov N A & Duraiswami R 2003 *SIAM Journal on Scientific Computing* **25**(4), 1344–1381.

Han Y, Gréhan G & Gouesbet G 2003 *Applied Optics* **42**(33), 6621–6629.

Han Y & Wu Z 2001 *Applied Optics* **40**, 2501–2509.

Hoekstra A G, Frijlink M, Waters L B F M & Sloot P M A 2001 *Journal of the Optical Society of America A* **18**, 1944–1953.

Humblet J 1943 *Physica* **10**(7), 585–603.

Jackson J D 1999 *Classical Electrodynamics* 3rd edn John Wiley New York.

Jauch J M & Rohrlich F 1976 *The Theory of Photons and Electrons* 2nd edn Springer New York.

Kahnert M 2005 *Journal of the Optical Society of America A* **22**(6), 1187–1199.

Khrapko R I 2001 *American Journal of Physics* **69**(4), 405.

Knöner G, Parkin S, Nieminen T A, Heckenberg N R & Rubinsztein-Dunlop H 2006 Measurement of refractive index of single microparticles.

Lock J A 2004a *Applied Optics* **43**(12), 2532–2544.

Lock J A 2004b *Applied Optics* **43**(12), 2545–2554.

Lorenz L 1890 *Videnskabernes Selskabs Skrifter* **6**, 2–62.

Maia Neto P A & Nussenzweig H M 2000 *Europhysics Letters* **50**, 702–708.

Mazolli A, Maia Neto P A & Nussenzveig H M 2003 *Proc. R. Soc. Lond. A* **459**, 3021–3041.

Mie G 1908 *Annalen der Physik* **25**(3), 377–445.

Minkowski H 1908 *Nachrichten von der Gesselschaft der Wissenschaften zu Göttingen, Mathematisch-Physikalische Klasse* **1908**, 53–111.

Mishchenko M I 1991 *Journal of the Optical Society of America A* **8**, 871–882.

Mishchenko M I, Videen G, Babenko V A, Khlebtsov N G & Wriedt T 2004 *Journal of Quantitative Spectroscopy and Radiative Transfer* **88**, 357–406.

Neves A A R, Fontes A, Pozzo L d, de Thomaz A A, Chillce E, Rodriguez E, Barbosa L C & Cesar C L 2006 *Optics Express* **14**(26), 13101–13106.

Nieminen T A, Heckenberg N R & Rubinsztein-Dunlop H 2001 *Journal of Modern Optics* **48**, 405–413.

Nieminen T A, Heckenberg N R & Rubinsztein-Dunlop H 2004 *Proc. SPIE* **5514**, 514–523.

Nieminen T A, Loke V L Y, Brańczyk A M, Heckenberg N R & Rubinsztein-Dunlop H 2006 *PIERS Online* **2**(5), 442–446.

Nieminen T A, Rubinsztein-Dunlop H & Heckenberg N R 2001 *Journal of Quantitative Spectroscopy and Radiative Transfer* **70**, 627–637.

Nieminen T A, Rubinsztein-Dunlop H & Heckenberg N R 2003*a Journal of Quantitative Spectroscopy and Radiative Transfer* **79-80**, 1019–1029.

Nieminen T A, Rubinsztein-Dunlop H & Heckenberg N R 2003*b Journal of Quantitative Spectroscopy and Radiative Transfer* **79-80**, 1005–1017.

Nieminen T A, Rubinsztein-Dunlop H, Heckenberg N R & Bishop A I 2001 *Computer Physics Communications* **142**, 468–471.

Pfeifer R N C, Nieminen T A, Heckenberg N R & Rubinsztein-Dunlop H 2006 *Proc. SPIE* **6326**, 63260H.

Ren K F, Gréhan G & Gouesbet G 1996 *Applied Optics* **35**, 2702–2710.

Simpson S H & Hanna S 2007 *Journal of the Optical Society of America A* **24**(2), 430–443.

Singer W, Nieminen T A, Gibson U J, Heckenberg N R & Rubinsztein-Dunlop H 2006 *Physical Review E* **73**, 021911.

Stewart A M 2005 *European Journal of Physics* **26**, 635–641.

Sun W, Pan S & Jiang Y 2006 *Journal of Modern Optics* **53**(18), 2691–2700.

Videen G 2000 *in* F Moreno & F González, eds, 'Light Scattering from Microstructures' number 534 *in* 'Lecture Notes in Physics' Springer-Verlag Berlin chapter 5, pp. 81–96.

Waterman P C 1971 *Physical Review D* **3**, 825–839.

White D A 2000*a Journal of Computational Physics* **159**, 13–37.

White D A 2000*b Computer Physics Communications* **128**, 558–564.

Wohland T, Rosin A & Stelzer E H K 1996 *Optik* **102**, 181–190.

Wong V & Ratner M A 2006 *Journal of the Optical Society of America B* **23**(9), 1801–1814.

Zambrini R & Barnett S M 2005 *Journal of Modern Optics* **52**(8), 1045–1052.